RSC Advances

ROYAL SOCIETY OF CHEMISTRY

www.rsc.org/advances

Electrochemical Exfoliation of Graphite for Producing Graphene Using Tetrasodium Pyrophosphate

Punith Kumar M K[#], Monika Nidhi[#] and Chandan Srivastava[#*]

[#]Dept. of Materials Engineering, Indian Institute of Science (IISc), Bangalore- 560012

*corresponding author

Abstract

An electrochemical exfoliation based synthetic methodology for producing graphene is provided. Eco-friendly and non-toxic tetrasodium pyrophosphate solution in which pyrophosphate anion acts as intercalating ion was used as electroactive media. Five different ion intercalation potentials were used. Characterization by the microscopy, X-ray diffraction, Raman spectroscopy and UV-Visible spectroscopic techniques confirmed that all the potentials produced nano to micrometer sized graphene sheets. No trace of graphene oxide was detected. It was observed that (i) an increase in the intercalation potential increased the graphene yield and (ii) defect density of graphene did not change significantly with change in the intercalation potential.

Keywords: Graphene, Electrochemical exfoliation, Tetrasodium pyrophosphate.

*Corresponding author. Tel: +91-80-22932834

E-mail address: csrivastava@materials.iisc.ernet.in (Chandan Srivastava)

Introduction:

Graphene is a single layer of sp^2 hybridized carbon atoms packed in a hexagonal honeycomb arrangement[1-3]. Because of its remarkable properties such as very high electrical and thermal conductivity and mechanical strength, graphene is being extensively investigated for their potential application in a variety of technological fields such as sensors[4,5], composite materials[2,6], solar cells[7], fuel cells[8,9] etc. After the first demonstration of possibility of isolating graphene from graphite[10], several efforts have been made to develop newer techniques such as solvothermal reduction[11], chemical synthesis[12], chemical vapor deposition[13], epitaxial growth[14] and electrochemical exfoliation[15] etc to achieve high-throughput of high quality graphene.

In the present work, we employed electrochemical exfoliation process to produce graphene from a graphite electrode. The electrochemical process derives its merit from the facts that it is a low cost, eco-friendly and non-equipment intensive technique[15,16]. Both anodic and cathodic electrochemical exfoliation processes are currently widely used to produce graphene by electrochemical exfoliation method[16,17]. Based on the ionic size and intercalating property, many organic and inorganic molecules are used to exfoliate graphite[18]. Gu *et al*[19] have proposed a high throughput method of producing high quality graphene sheets by liquid phase exfoliation of worm like exfoliated graphite using concentrated sulphuric acid and hydrogen peroxide.[19] Use of sulphate based compounds like sulphuric acid or inorganic sulphate salts leads to intercalation of sulphate anion within the carbon layers in graphite. Ionic size of the SO_4^{2-} anion is 0.46 nm which is larger than the interlayer spacing between the graphitic layer ie., 0.335 nm.[20] The intercalated SO_4^{2-} ion therefore weakens the bond between the graphitic layers and leads to the exfoliation of graphite into separate graphene layers. Majority of the intercalating molecules like acids, bases and ionic liquids which are being used however are highly aggressive, corrosive and

eco-toxic in nature. In the interest of environment and personnel safety, use of these molecules therefore should be discouraged both in laboratory and industrial scale processes that produce graphene. Hence, there exists a need for identifying and developing exfoliation processes that employ eco-friendly and non-toxic molecules. Some "green" approaches to produce graphene-based materials have already been reported in the literature. In one of the approaches, Parvez *et al*[21] have electrochemically exfoliated graphite using aqueous inorganic salt solutions like ammonium sulphate, sodium sulphate and potassium sulphate to produce highly conductive graphene layers.[21] In yet another approach, Lee *et al*[22] have anodically exfoliated graphite in poly(sodium-4-styrenesulfonate) electrolyte using simple DC source and demonstrated the influence of exfoliated graphene on enhancement of electrochemical performance of Li ion battery electrodes.[22]

Here we demonstrate the use of non-toxic tetrasodium pyrophosphate (TSPP) compound as an electroactive media to exfoliate graphite rod at different intercalation potentials to produce graphene. Pyrophosphate ion is non-toxic and biocompatible[23,24]. It is common in sea food, tooth paste and is extensively used as a food additive. Structure of Tetrasodium pyrophosphate (TSPP) is shown in Fig. 1(a). Tetrasodium pyrophosphate anion leads to anodic exfoliation process because of the intercalation of bulky pyrophosphate anion molecule within the graphitic layers. Intercalation induces strain between the layers and expands the graphite anode facilitating exfoliation as illustrated in Fig. 1(b).

Experimental:

Graphite rod was electrochemically exfoliated using Chronoamperometry technique with CHI-640E electrochemical workstation (US make). Three electrode system with two graphite rods (Alfa Aesar, INDIA) and platinum foil were used as cathode, anode and quasi-reversible

reference electrode respectively. Five separate electrochemical exfoliation experiments were carried out for 8 hrs using 3V, 4V, 5V 6V and 7V intercalation potentials in 0.03M Tetrasodium pyrophosphate aqueous electroactive media (pH = 10.67) prepared using Millipore water. After electrochemical exfoliation, the exfoliated product was sonicated for 1hr for vibration induced exfoliation in order to get finer suspension. The unexfoliated graphitic particles also present in the solution along with finer graphene were separated by centrifuging the suspension at 1000rpm for 10min. Fine suspension in the upper part of the centrifuge tube was then isolated and washed with water and subjected to characterization.

X-ray diffraction (XRD) profiles from graphene samples deposited on glass substrate were obtained by using X-pert pro X-ray diffractometer employing a Cu Kα radiation (λ = 0.1540 nm) source. Raman spectrums from the exfoliated samples were obtained using microscope setup (HORIBA JOBIN YVON, Lab RAM HR) consisting of Diode-pumped solid-state laser operating at 532 nm with a charge coupled detector. UV-Visible absorption spectroscopic experiments were carried in 700 to 200 nm wavelength range using Perkin Elmer (Lambda 35) UV-Vis Spectrometer. Scanning electron micrographs of graphene samples prepared on silica substrate were acquired using JOEL – JEM – 1200 – EX II Scanning electron microscope (SEM) operating at 20 kV. A 300 keV field emission FEI Tecnai F-30 transmission electron microscope (TEM) was used for obtaining TEM bright field images of exfoliated graphene samples. Samples for the TEM based analysis were prepared by drop drying graphene dispersion on a carbon coated copper grid. Atomic force microscopy (AFM) experiments were carried at room temperature using Nanosurf AFM instrument (Switzerland). Graphene-ethanol dispersion was drop dried over silica substrate for the AFM based analysis.

Result and Discussion:

XRD profiles obtained from graphite rod and graphene samples exfoliated at different intercalation potentials are shown in Fig 2. XRD profile obtained from unexfoliated graphite shows four distinct peaks at 26.75º, 43.35º, 44.67º and 54.67º 2θ corresponding respectively to the (0 0 2), (1 0 0), (1 0 1) and (0 0 4) graphitic planes[25]. XRD profiles from all the exfoliated products however revealed a broad peak centered at the 2θ value of ~25º which is the typical diffraction signature of few layered graphene sheets[26]. The XRD profiles of the exfoliated graphene also show a sharp peak overlapping the broad hump. This sharp peak is (002) reflection from the graphitic structure[16]. The broad peak illustrates disordering of the initial graphitic structure and a reduction in number of stacked layer in the electrochemically exfoliated graphene[16]. Also, the absence of graphene oxide characteristic peak around 14º 2θ values indicated the presence of only graphene layers in the exfoliated samples. Use of high exfoliation potentials can lead to oxidation. The absence of peak corresponding to the graphene oxide in the XRD curve however illustrates that if graphene oxide is present then it is in negligible amount in the exfoliated samples.

The absorption of UV-Vis light depends on the functional groups present in the materials being investigated hence UV-Vis absorption spectroscopy is a useful tool to distinguish between graphene and graphene oxide which basically differ in functionalities attached to the parental carbon structure. The recorded UV-Vis spectra for the exfoliated graphene samples are shown in Fig. 3(a). The maximum absorption (λ_{max}) at 270 nm which corresponds to $\pi \rightarrow \pi^*$ transition of the aromatic C-C bonds in graphene was observed for all the exfoliated samples. The absence of graphene oxide characteristic absorption peak around 230 nm confirmed that all the exfoliated samples contained only reduced graphene sheets[16,27]. The insert in Fig. 3(a) clearly shows the

absence of peak ~230 nm. The absence of graphene oxide peak in Fig. 3(a) supports the XRD results about the presence of negligible amount of graphene oxide in the exfoliated sample. It can be observed in Fig. 3(a) that the absorption intensity is increased with increase in the exfoliation potential. It should be noted that equal volumes of the ethanol dispersion of graphene from different exfoliation experiments were used for the UV-Vis absorption measurement. The variations in absorption intensity therefore clearly illustrates that the concentration of graphene in the suspension and thus its yield depends on the voltage that was used for the exfoliation process. In order to determine the concentration of exfoliated graphene samples, the absorption coefficient (α) was first determined experimentally. Absorption coefficient is an important parameter in characterizing concentration using the Lambert–Beer law[28] ($A/l = \alpha C$ where, A is absorption peak intensity; l is path length; C is concentration and α is the absorption coefficient). Graphene dispersions in ethanol with known concentrations were prepared. Absorbance per unit path length was then measured at λ_{660} nm. Relationship between absorption per unit length and known graphene concentrations is shown as a plot in Fig. 3(b). Slope of the straight line fit through the data points in Fig. 3(b) provided the absorption co-efficient value of $\alpha = 2421$ ml mg^{-1} m^{-1}. This absorption coefficient value was then used to determine the unknown concentration of the graphene dispersions obtained from different exfoliation experiments using the Lambert-Beer law and the value of absorption per unit length at λ_{660} nm in the UV-Vis profiles in Fig. 3(a). Concentration of graphene in the exfoliated dilute graphene dispersions were found to be 9.87 µg ml^{-1}, 11.18 µg ml^{-1}, 12.54 µg ml^{-1}, 17.67 µg ml^{-1} and 23.57 µg ml^{-1} for 3V, 4V, 5V, 6 V and 7 V respectively. Therefore an increase in the exfoliation potential increased the yield of graphene.

Raman spectra obtained from graphite and electrochemically exfoliated samples are given in Fig. 4(a). The Raman spectra of all the samples revealed three major peaks: D band at ~1361cm^{-1} corresponding to sp^3 defects, G band around ~1580 cm^{-1} corresponding to the phonon mode in-plane vibration of sp^2 carbon atoms and 2D band at ~2700 cm^{-1} corresponding to the two phonon lattice vibration[27,29,30]. A slight shift in the 2D band position of the exfoliated samples towards lower wave number as compared to the 2D peak position of graphite and a considerable intensity of the 2D peak observed in Raman spectra of exfoliated samples as shown in Fig. 4(b) collectively confirmed the presence of few layer graphene in the exfoliated samples[26]. The intensity ratio between D and G peak i.e., I_D/I_G gives the defect density of the graphitic structure[30]. The I_D/I_G ratios of graphite and graphene samples produced at different intercalation voltages are tabulated in Table 1. It is apparent from table 1 that the defect density ratio of graphene did not differ significantly from the defect density of the graphite rod from which it was exfoliated for all the exfoliation potentials and the exfoliation potential also did not significantly effect on the defect density of the exfoliated product. One important observation that can be made from the Fig. 4(a) is the appearance of a shoulder near 1615 cm^{-1} in the G-band peak as illustrated in Fig. 4(c) which plots the fitted curves obtained after de-convolution of the G-band peak and its shoulder. This shoulder peak is identified as the D' band. It has been shown that this peak appears in few-layer graphene and is due to the presence of defects in the sp^2 carbon lattice[31-33]. D' peak has also been reported for metallic CNT samples with defects[34]. Relative difference in the intensity of the D' peak between the graphene samples exfoliated at different voltages indicates towards the effect of exfoliation potential on the defects in the sp^2 carbon lattice of the graphene samples.

Representative SEM images of graphene samples dispersed over silica wafer are shown in Fig. 5. The SEM micrographs reveal large, irregular and well separated graphene sheets with dimensions from nano to micron scale. Representative TEM bright field image of exfoliated graphene samples are shown in Fig. 6. TEM images clearly reveal the presence of isolated few layer graphene sheets in the exfoliated samples. Thickness of the exfoliated graphene sheets was investigated using the AFM technique. Representative AFM topographical images of graphene sheets exfoliated at different voltages is shown in Fig. 7. The Z-height profiles obtained from AFM images revealed that the graphene flakes exfoliated using 3-7 V had a thickness of 5±2.3nm, 4.5±1.3nm, 5.9±1.0nm, 6.3±0.9, 5.7±1.5nm respectively. This result illustrated that the as-exfoliated samples contained few layer graphene sheets for all the exfoliation voltages. TEM and AFM images and thickness measurement results additionally illustrated that the as-synthesized graphene sheets were not agglomerated.

Conclusions:

In the present work graphene sheets were successfully synthesized by electrochemical exfoliation technique using Tetrasodium pyrophosphate. Five different ion intercalation potentials were employed for exfoliation. The broad peak obtained in XRD pattern around ~25º 2θ value indicated the presence of graphene in the exfoliated samples. The UV-Vis spectra of all the samples revealed only one peak around 270 nm which confirmed the presence of pure graphene and absence of graphene oxide in the exfoliated samples. Intense 2D peak in Raman spectra revealed that exfoliated samples contains few layer graphene sheets. Two important observations made were (a) an increase in the intercalation potential increased the yield of the graphene and (b) the defect density of graphene remained independent of the intercalation potential.

Acknowledgement

Authors acknowledge research funding from Joint Advanced Technology Program (JATP), Indian Institute of Science, Bangalore, India. The authors deeply acknowledge the facilities available in Professor Praveen C Ramamurthy Laboratory, Materials Engineering, Indian Institute of Science, Bangalore.

References:

1. A. K. Geim and K. S. Novoselov, *Nat. Mater.,* 2007, **6**(3), 183-191.

2. Sasha Stankovich, Dmitriy A. Dikin, Geoffrey H. B. Dommett, Kevin M. Kohlhaas, Eric J. Zimney, Eric A. Stach, Richard D. Piner, SonBinh T. Nguyen and Rodney S. Ruoff, *Nature*, 2006, **442**, 282-286.

3. D. H. Nagaraju and G. S. Suresh, *ECS Electrochemistry Letters,* 2012, **1**(3), F21-F23.

4. Long Yang, Guangcan Wang, Yongjun Liu and Min Wang, *Talanta*, 2013, **113**, 135-141.

5. Wenjing Yuan and Gaoquan Shi, *J. Mater. Chem. A*, 2013, **1**, 10078-10091.

6. Wen Shen, Yuqi Yu, Jiangnan Shu and Hua Cui, *Chem. Commun.*, 2012, **48**, 2894-2896.

7. Ching-Yuan Su, Ang-Yu Lu, Yanping Xu, Fu-Rong Chen, Andrei N. Khlobystov, and Lain-Jong Li, *ACS Nano*, 2011, **5**(3), 2332-2339.

8. Hyun-Jung Choia, Sun-Min Junga, Jeong-Min Seoa, Dong Wook Changb, Liming Daic and Jong-Beom Baek, *Nano Energy*, 2012, **1**, 534-551.

9. Minmin Liu, Ruizhong Zhang and Wei Chen, *Chem. Rev.* 2014, **114**, 5117-5160.

10. K. S. Novoselov, A. K. Geim, S. V. Morozov, D. Jiang, Y. Zhang, S. V. Dubonos, I. V Grigorieva and A. A. Firsov, *Science*, 2004, **306**, 666-669.

11. Pengyu Dong, Yuhua Wang, Linna Guo, Bin Liu, Shuangyu Xin, Jia Zhang, Yurong Shi, Wei Zeng and Shu Yin, *Nanoscale*, 2012, **4,** 4641-4649.

12. Siegfried Eigler, Michael Enzelberger-Heim, Stefan Grimm, Philipp Hofmann, Wolfgang Kroener, Andreas Geworski, Christoph Dotzer, Michael Röckert, Jie Xiao, Christian Papp, Ole Lytken, Hans-Peter Steinrück, Paul Müller and Andreas Hirsch, *Adv. Mater.*, 2013, **25,** 3583-3587.

13. Subash Sharma, Golap Kalita, Ryo Hirano, Sachin M. Shinde, Remi Papon, Hajime Ohtani and Masaki Tanemura, *Carbon*, 2014, **72**, 66-73.

14. S. P. Cooil, F. Song, G. T. Williams, O. R. Roberts, D. P. Langstaff, B. Jørgensen, K. Høydalsvik, D. W. Breiby, E. Wahlstrom, D. A. Evans and J. W. Wells, *Carbon*, 2012, **50,** 5099-5105.

15. Jilei Liu, Huanping Yang, Saw Giek Zhen, Chee Kok Poh, Alok Chaurasia, Jingshan Luo, Xiangyang Wu, Edwin Kok Lee Yeow, Nanda Gopal Sahoo, Jianyi Lin and Zexiang Shen, *RSC Advances*, 2013, **3**, 11745-11750.

16. Murat Alanyalioglu, Juan Jose Segura, Judith Oro-Sole and Nieves Casan-Pastor, *Carbon*, 2012, **50**, 142-152.

17. Yingchang Yang, Xiaobo Ji, Xuming Yang, Chiwei Wang, Weixin Song, Qiyuan Chen and Craig E. Banks, *RSC Advances*, 2013, **3**, 16130-16135.

18. Jilei Liu, Chee Kok Poh, Da Zhan, Linfei Lai, San Hua Lim, Liang Wang, Xiaoxu Liu, Nanda Gopal Sahoo, Changming Li, Zexiang Shen and Jianyi Lin, *Nano Energy,* 2013, **2,** 377-386.

19. Wentian Gu, Wei Zhang, Xinming Li, Hongwei Zhu, Jinquan Wei, Zhen Li, Qinke Shu, Chen Wang, Kunlin Wang, Wanci Shen, Feiyu Kang and Dehai Wu*, J. Mater. Chem.,* 2009, **19,** 3367–3369.

20. Khaled Parvez, Rongjin Li, Sreenivasa Reddy Puniredd, Yenny Hernandez, Felix Hinkel, Suhao Wang, Xinliang Feng and Klaus Mullen 2013 *ACS Nano.,* **7,** 3598-3606.

21. Khaled Parvez, Zhong-Shuai Wu, Rongjin Li, Xianjie Liu, Robert Graf, Xinliang Feng and Klaus Müllen, *J. Am. Chem. Soc.,* 2014, **136,** 6083−6091.

22. Seung-Hun Lee, Seung-Deok Seo, Yun-Ho Jin, Hyun-Woo Shim and Dong-Wan Kim, *Electrochem. Commun.,* 2010, **12,** 1419–1422

23. Nadia Marino, Oluwatayo. F. Ikotun, Miguel Julve, Francesc Lloret, Juan Cano, and Robert P. Doyle, *Inorg. Chem.*, 2011, **50**, 378-389.

24. Guzman Sanchez, David Curiel, Witold Tatkiewcz, Imma Ratera, Alberto Tarraga, Jaume Veciana and Pedro Molina, *Chem. Sci.*, 2014, **5**, 2328-2335.

25 Z.Q. Li, C.J. Lu, Z.P. Xia, Y. Zhou and Z. Luo, *Carbon*, 2007, **45,** 1686-1695.

26. Liyong Niu, Mingjian Li, Xiaoming Tao, Zhuang Xie, Xuechang Zhou, Arun P. A. Raju, Robert J. Young and Zijian Zheng, *Nanoscale*, 2013, **5**, 7202-7208.

27. J. I. Paredes, S. Villar-Rodil, P. Solis-Fernandez, A. Martinez-Alonso and J. M. D. Tascon, *Langmuir*, 2009, **25(10)**, 5957-5968.

28. Mustafa Lotya, Yenny Hernandez, Paul J. King, Ronan J. Smith, Valeria Nicolosi, Lisa S. Karlsson, Fiona M. Blighe, Sukanta De, Zhiming Wang, I. T. McGovern, Georg S. Duesberg and Jonathan N. Coleman *J. Am. Chem. Soc.,* 2009, **131** 3611-3620.

29. Andrea C. Ferrari and Denis M. Basko, *Nat. Nanotec.*, 2013, **8**, 235-246.

30. L.M. Malarda, M.A. Pimenta, G. Dresselhaus and M.S. Dresselhaus, *Phys Rep*, 2009, **473**, 51-87.

31. C. N. R. Rao, Kanishka Biswas, K. S. Subrahmanyama and A. Govindaraj, *J. Mater. Chem.,* 2009, **19,** 2457–2469.

32. Yung Ho Kahng, Sangchul Lee, Woojin Park, Gunho Jo, Minhyeok Choe, Jong-Hoon Lee, Hyunung Yu, Takhee Lee and Kwanghee Lee, *Nanotechnology*, 2012, **23**, 075702 (1-9).

33. Matteo Bruna and Stefano Borini, *Phys. Rev. B.,* 2010, **81,** 125421(1-7).

34. Andrea C. Ferrari, *Solid State Commun.,* 2007, **143,** 47–57.

Figure Captions:

Fig 1: (a) Structures of Tetrasodium pyrophosphate (TSPP) molecule and (b) a schematic showing the mechanism of graphene exfoliation in presence of TSPP.

Fig. 2: X-ray diffraction profiles obtained from graphite and graphene exfoliated at different intercalation potential.

Fig 3: (a) UV-Visible absorption spectra of electrochemically exfoliated graphene sample at different intercalation potential. Insert shows the profile between 200 to 300 nm^{-1}, (b) Optical absorbance (λ=660nm) per unit length (A/l) as a function of concentration of graphene. Insert text shows Lambert-Beer law with an absorption co-efficient α = 2421 ml mg^{-1} m^{-1}.

Fig 4: (a) Raman spectra of graphite and graphene prepared at different potentials, (b) Raman spectra re-ploted to show only the 2D peak, (c) Raman spectra showing the G and D' band peaks. The G and D' band peaks were deconvoluted using peak fitting routine.

Fig 5: SEM micrographs of graphene exfoliated at different intercalation potential.

Fig 6: TEM bight field micrographs of graphene prepared by electrochemical exfoliation process at different intercalation potential.

Fig 7: AFM topographical images of graphene synthesized at 3V, 4V, 5V, 6V and 7V intercalation potential.

Table caption:

Table 1: Defect density ratio (I_D/I_G) of graphite and graphene samples calculated from Raman spectra

Sample	G	3V	4V	5V	6V	7V
I_D/I_G	0.9719	0.9754	1.0740	0.9962	0.9964	1.0707

Table 1

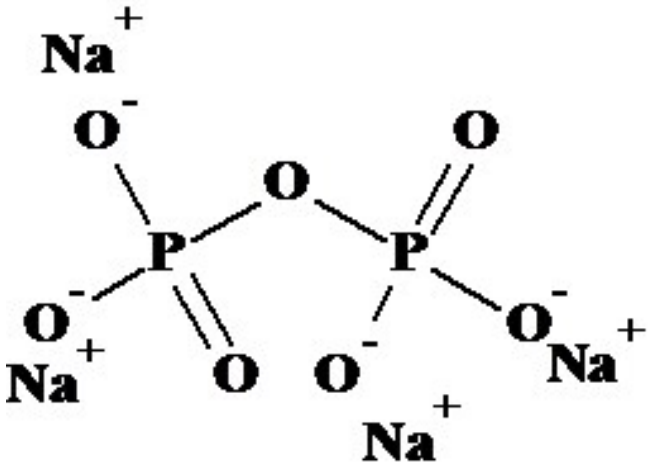

(a)

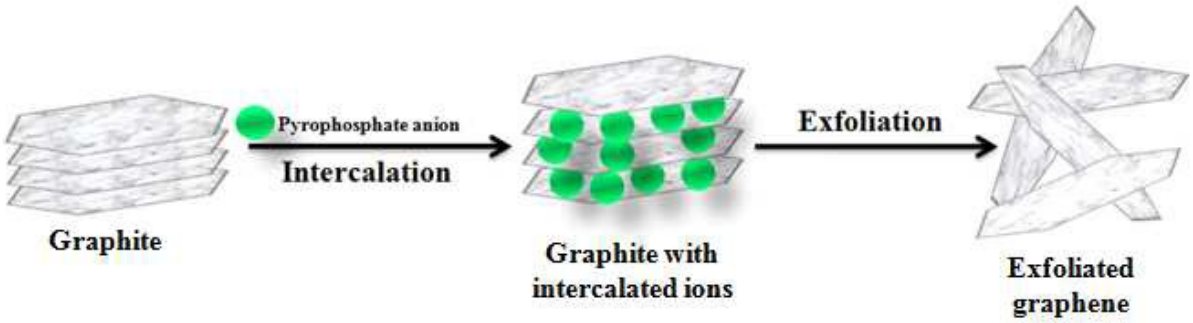

(b)

Figure 1

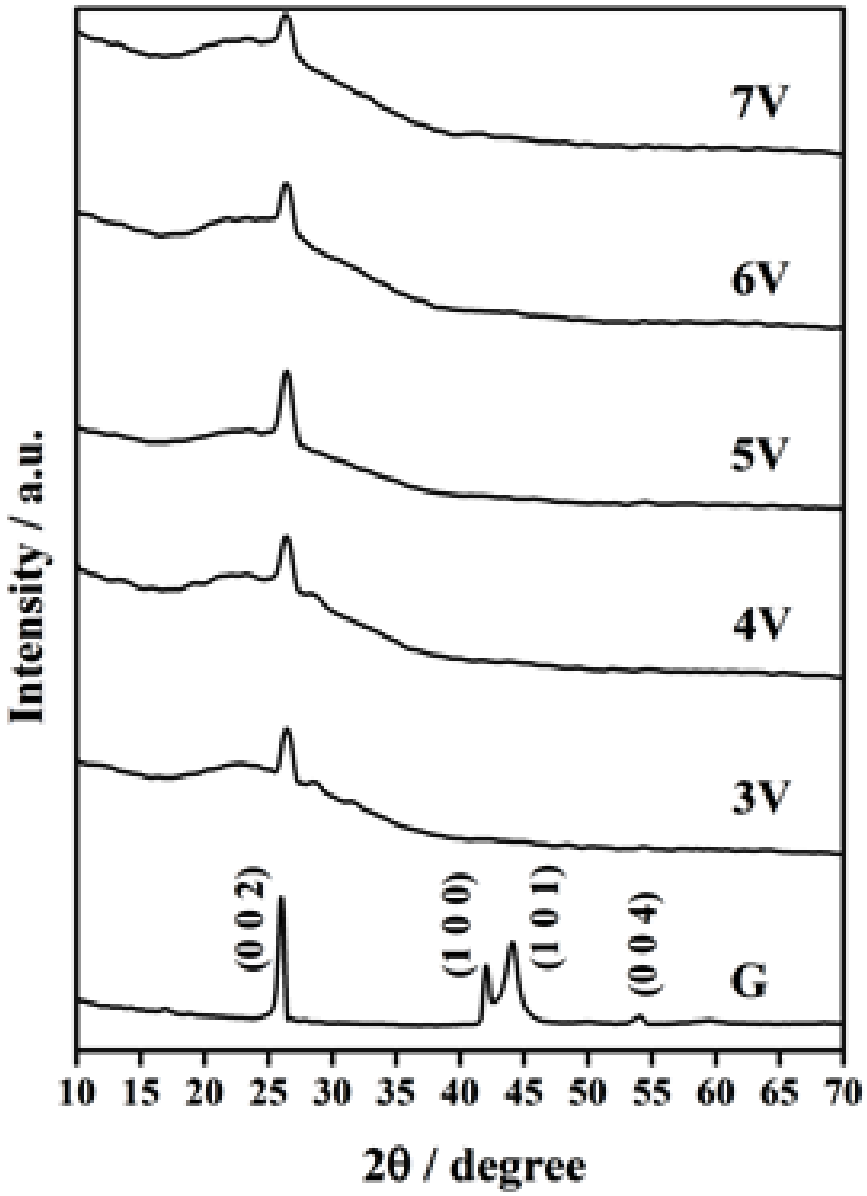

Figure 2

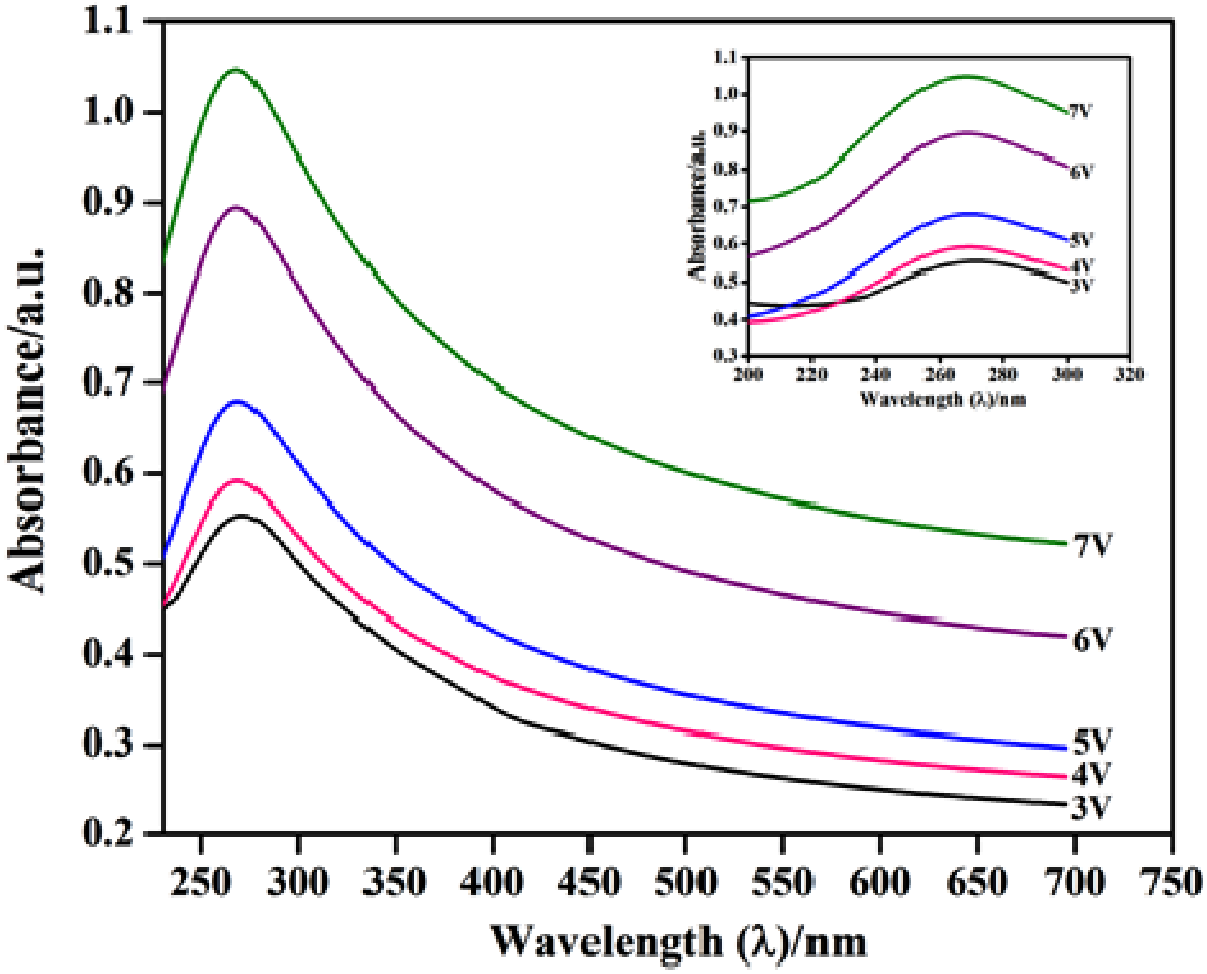

Figure 3(a)

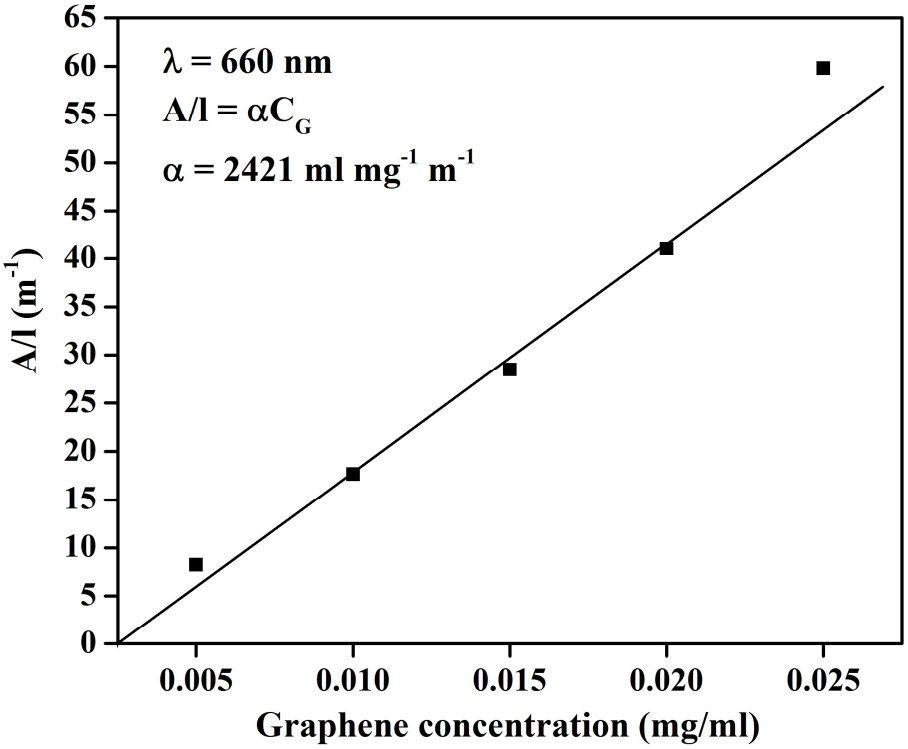

Figure 3(b)

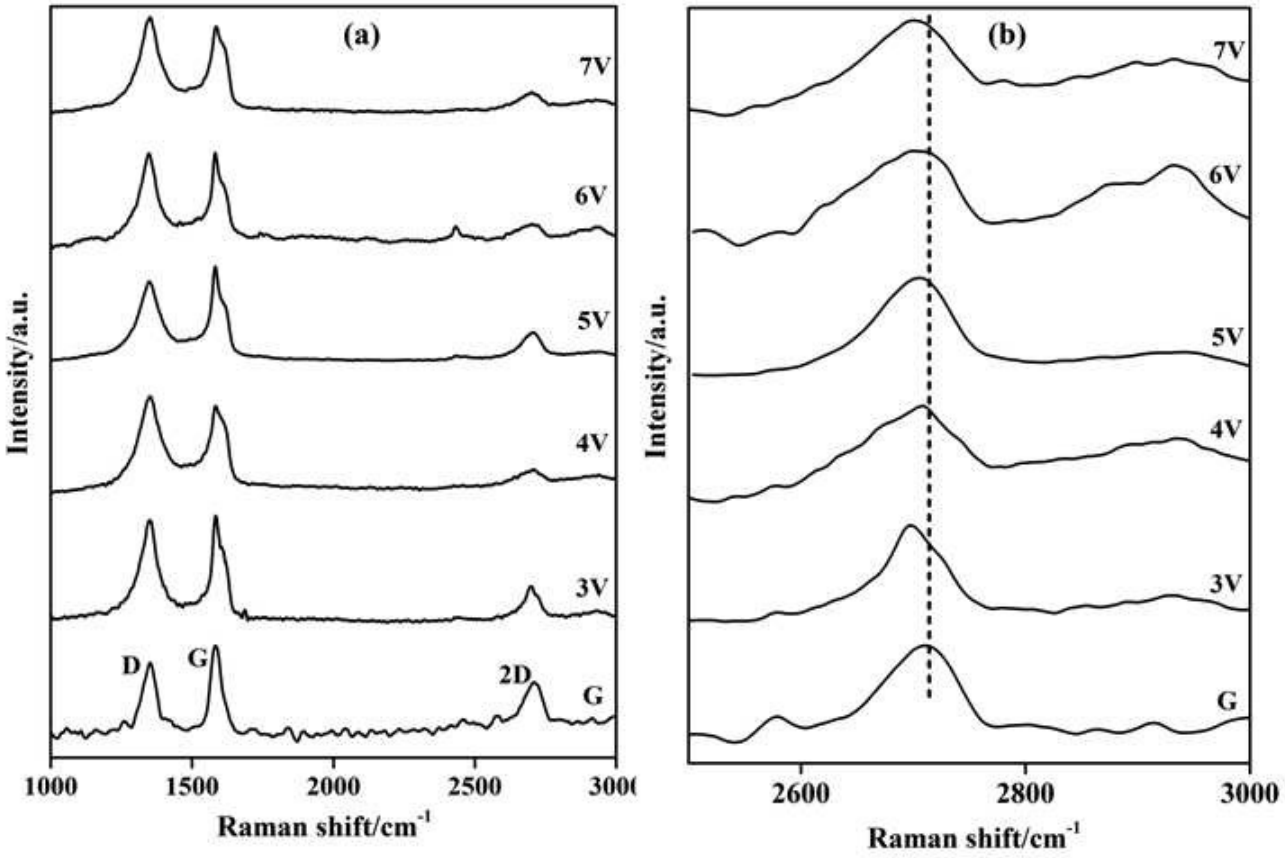

Figure 4(a) and 4(b)

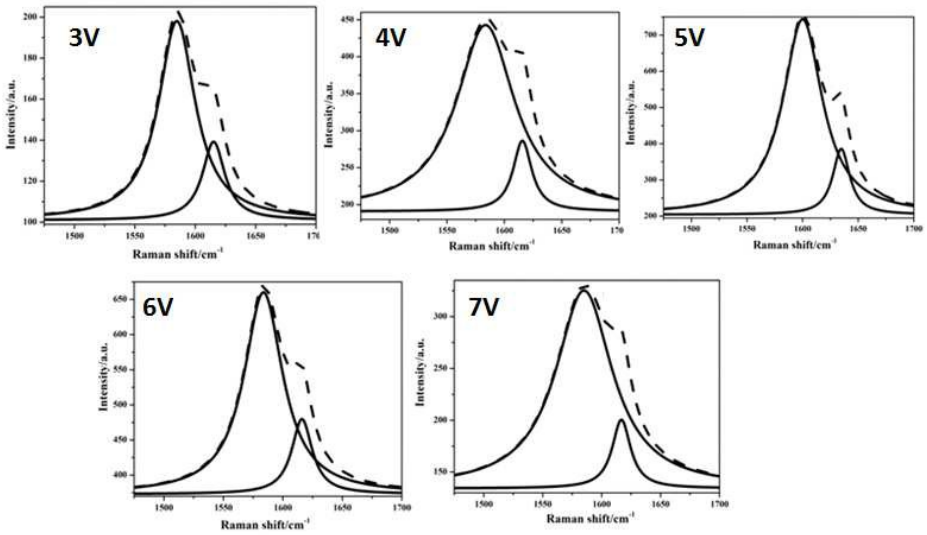

Figure 4(c)

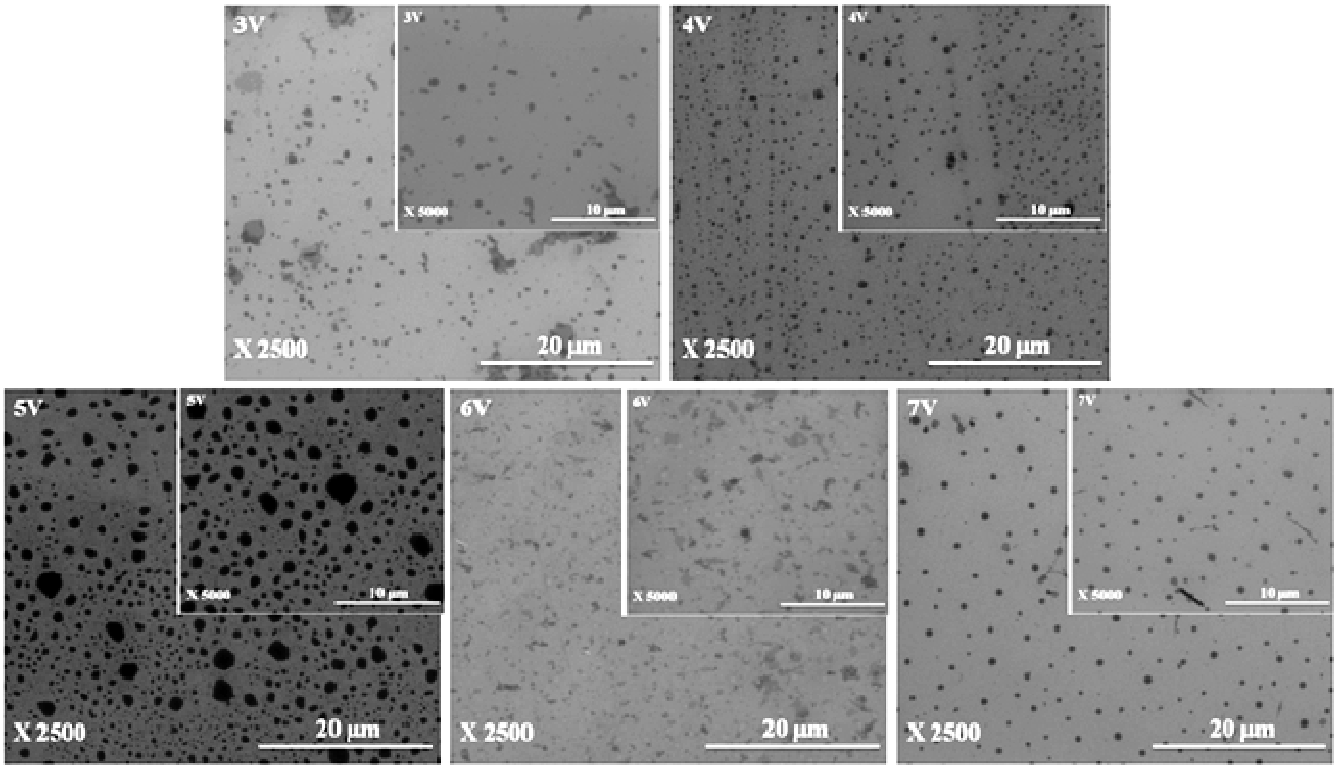

Figure 5

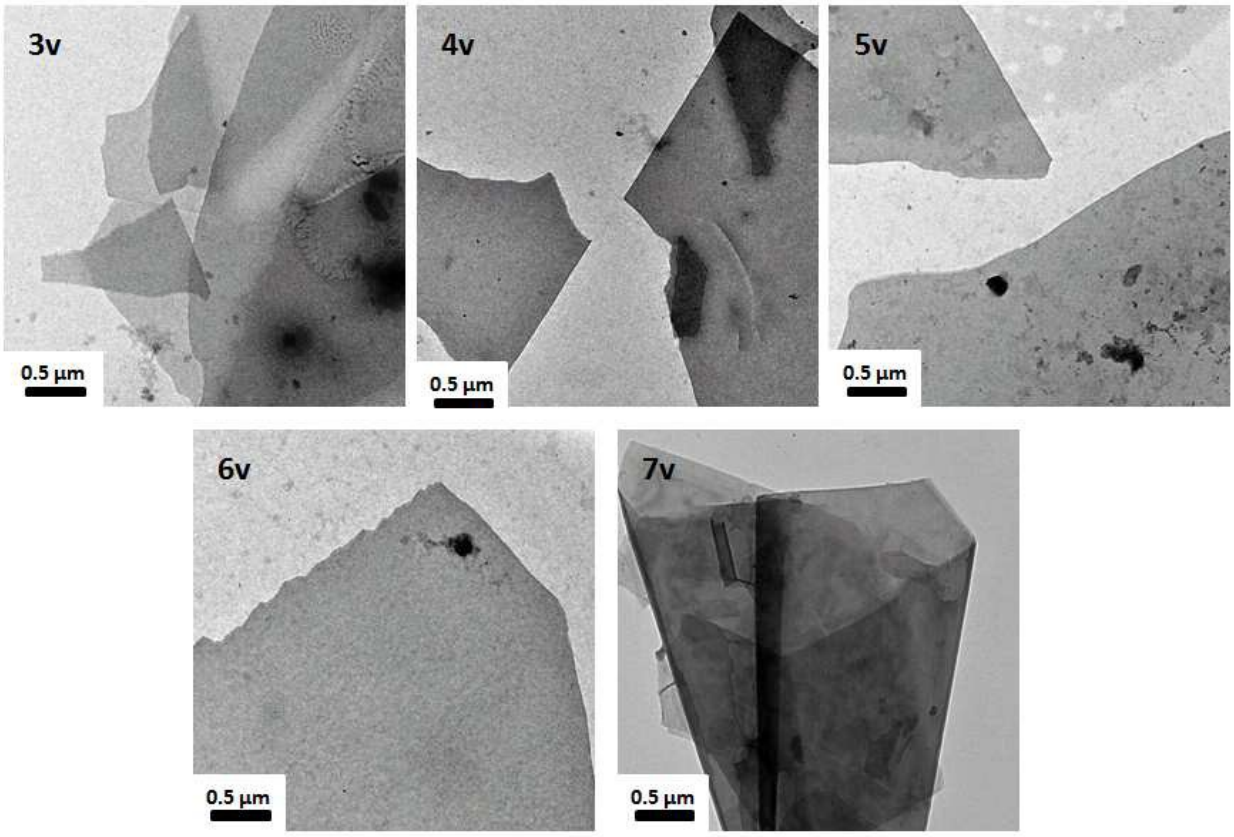

Figure 6

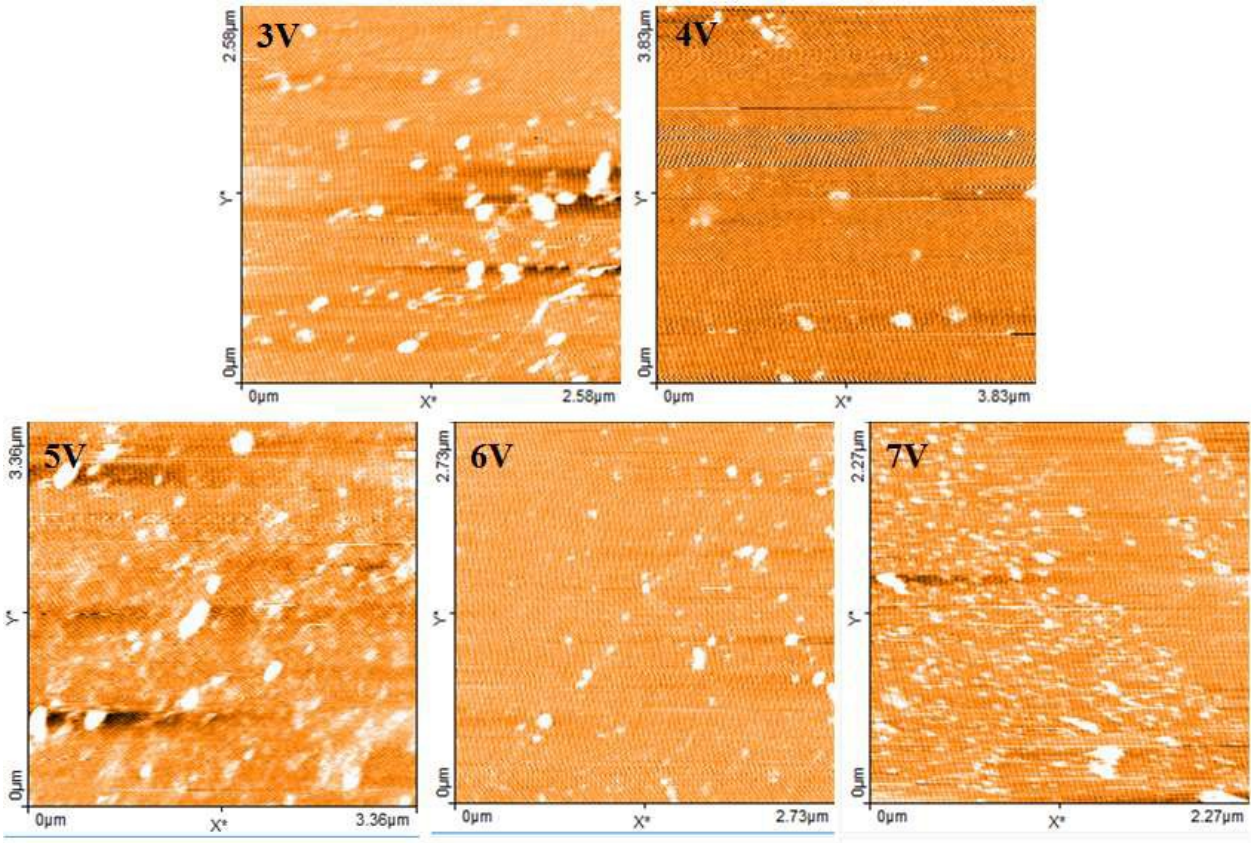

Figure 7